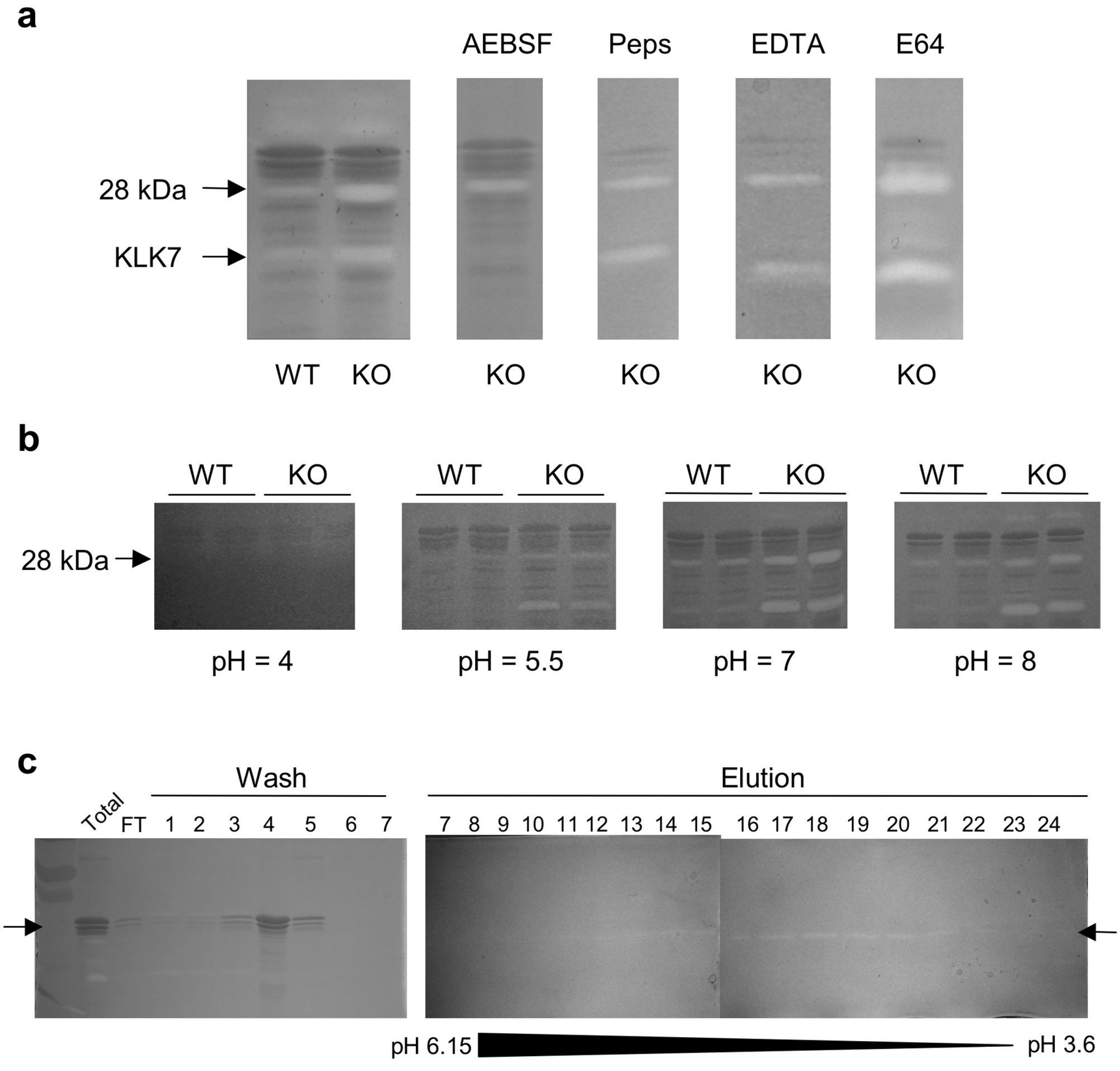

Supplementary Figure 1 - Characterization of the 28 kDa protease and affinity purification on SbTI affinity column

(a) Inhibitor sensitivity of the 28 kDa protease. Proteolytic activity of the 28 kDa in normal (WT) and *Spink5*$^{-/-}$ (KO) mouse epidermis was analyzed by casein gel zymography. The 28 kDa proteolytic activity is detected in WT epidermis but is more intense in KO samples. This activity is not inhibited by different class-specific inhibitors used: AEBSF (serine protease inhibitor), pepstatin (aspartate protease inhibitor), EDTA (metalloprotease inhibitor) and E64 (cystein protease inhibitor). **(b)** pH-dependent activity of the 28 kDa protease. Epidermal samples from 2 WT and 2 KO were analyzed on casein gel zymography performed at pH 4, 5.5, 7 and 8. The 28 kDa protease activity is maximal at pH 7, and decreases with acidification. A residual activity is visible at pH 5.5, but none remains at pH 4.4. **(c)** Purification of the 28 kDa on SbTI affinity column. The chromatography column was loaded with acetic acid extracted epidermal proteins, washed, and elution was performed with an acidic pH gradient. Each collected fraction was analyzed by casein gel zymography. “Total” corresponds to the unpurified fraction, “FT” refers to the flow through of the column. The 28 kDa protease activity (arrow) is detected from elution fractions 11 to 21. These fractions, devoid of any other visible proteolytic activity, were pooled and submitted to mass spectrometry analysis.

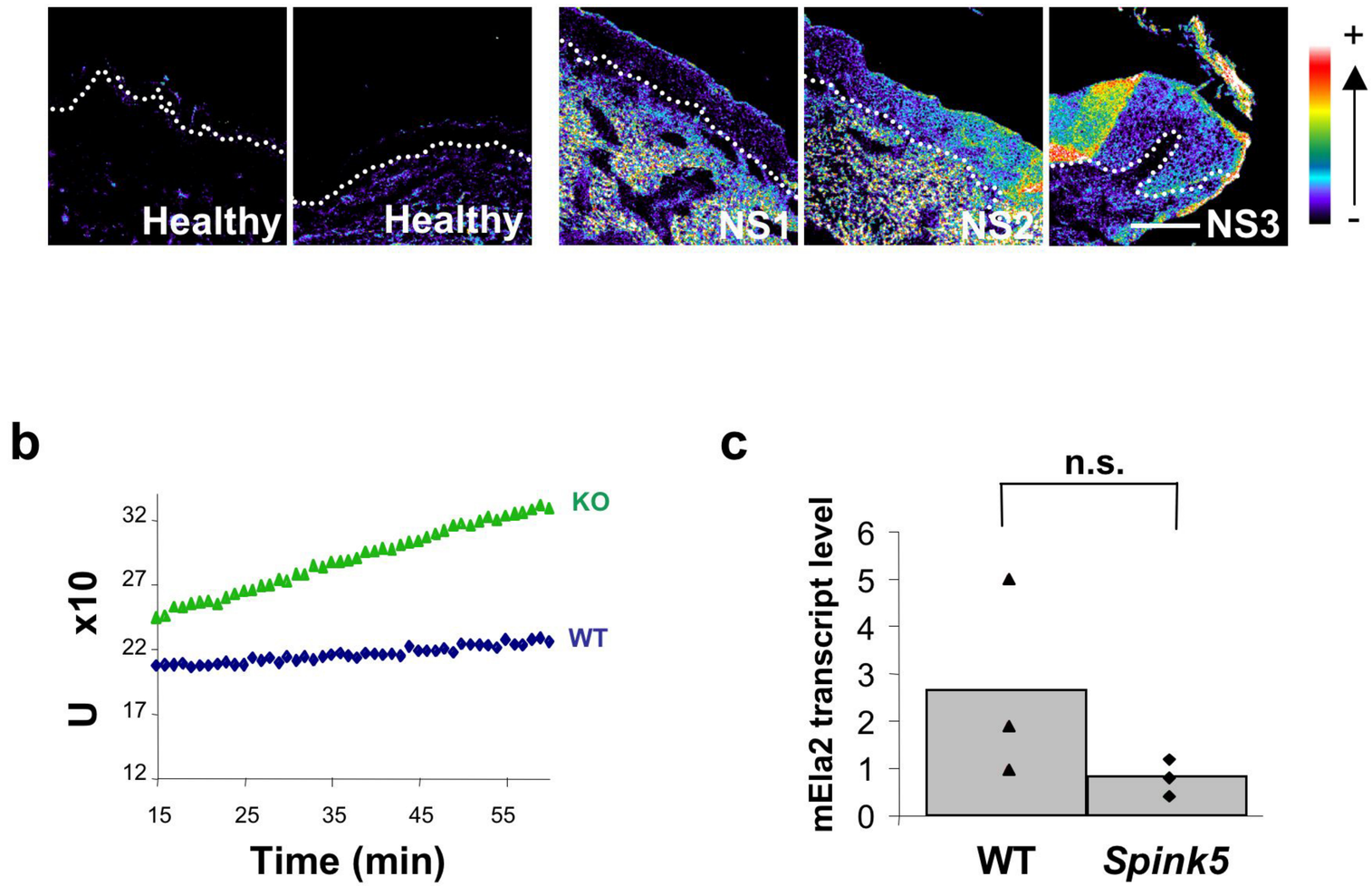

Supplementary Figure 2 - Elastolytic activity in NS patient skin and in *Spink5*$^{-/-}$ epidermis

(**a**) *In situ* zymography analysis of 2 healthy and 3 Netherton syndrome patients (NS1 to NS3) skins. Elastolytic activity was faintly detected in the granular layer as well as in the SC of normal skin. Elastolytic activity is strongly increased in the NS epidermis. The color gradient represents the intensity values of the fluorescence signals ranging from 0 (dark) to 255 (white). The dotted line represents the basal membrane of the epidermis. Scale bar: 500 μm. (**b**) Quantification of elastolytic activity in wild-type (WT) and *Spink5*$^{-/-}$ (KO) epidermal extracts. Elastolytic activity measured by the degradation velocity of FITC-conjugated elastin is increased 5.3 times in KO extracts compared to WT. This result is representative of 3 independent experiments. **(c)** Relative *Ela2A* transcript levels in WT and *Spink5*$^{-/-}$ mice skin using quantitative RT-PCR with *Ela2* primers. Transcript levels were normalized to *Hprt* abundance. Charts represent each individual value (dots) and average (histograms). n.s., not significant.

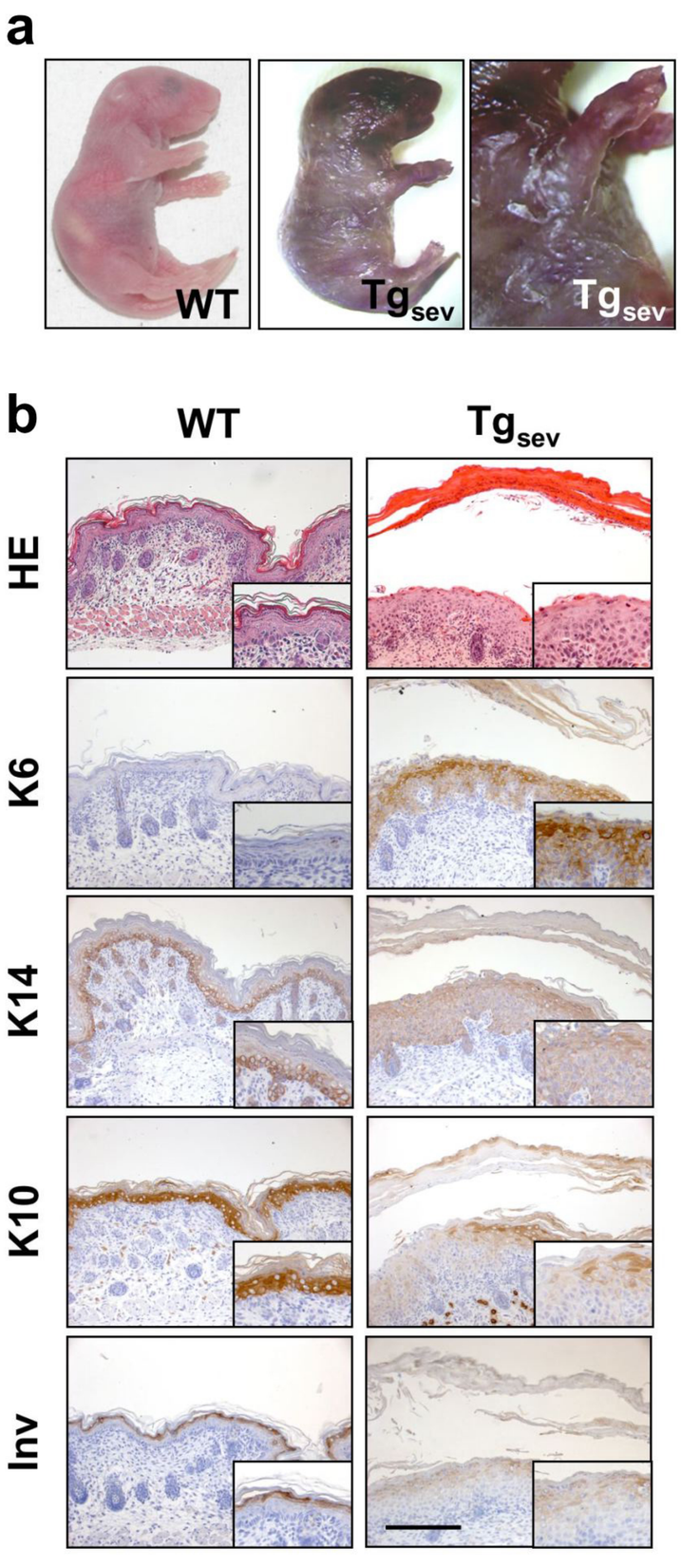

Supplementary Figure 3 - Phenotype and skin analysis of the severely affected Tg-ELA2 (Tg_{sev})

(a) The transgenic animal was found dead at birth. Macroscopic examination showed a generalized erythema and massive scales. **(b)** Hematoxylin and eosin (HE) staining of the Tg-ELA2 showed an acanthotic epidermis with hypogranulosis and prominent hyperkeratosis, and stratum corneum often detached from the underlying epidermis. Immunohistochemical analysis revealed that the hyperproliferation marker Keratin 6 (K6) was highly expressed in the suprabasal layers of Tg-$ELA2_{sev}$ epidermis. The basal marker Keratin 14 (K14) was extended to the suprabasal compartment. The Keratin 10 (K10) and involucrin (Inv) immunostainings were markedly reduced in Tg-$ELA2_{sev}$ epidermis. **(c)** Immunofluorescence of WT and Tg-$ELA2_{sev}$ skin sections with anti-FLAG antibody revealed a high-level and patchy transgene expression in the granular layer and stratum corneum of Tg-$ELA2_{sev}$. **(d)** *In situ* zymography analysis of skin cryosections showed a high elastolytic activity in the granular layer and stratum corneum of Tg-$ELA2_{sev}$. Note that stratum corneum is attached to the underlying epidermis on this area. **(e)** Filaggrin immunostaining was massively reduced in Tg-$ELA2_{sev}$ epidermis. **(f)** Nile red staining of WT epidermis showed well formed yellow lines. In contrast, the Tg-$ELA2_{sev}$ SC displayed no lamellar structure but numerous lipid droplets in intra and extracellular spaces. Note the thickness of the SC (brackets) in the transgenic epidermis compared to the WT. bars: b and e: 200 μm; c and d: 50 μm; f: 20 μm. Higher magnifications of each panel in b and e are shown as insets.

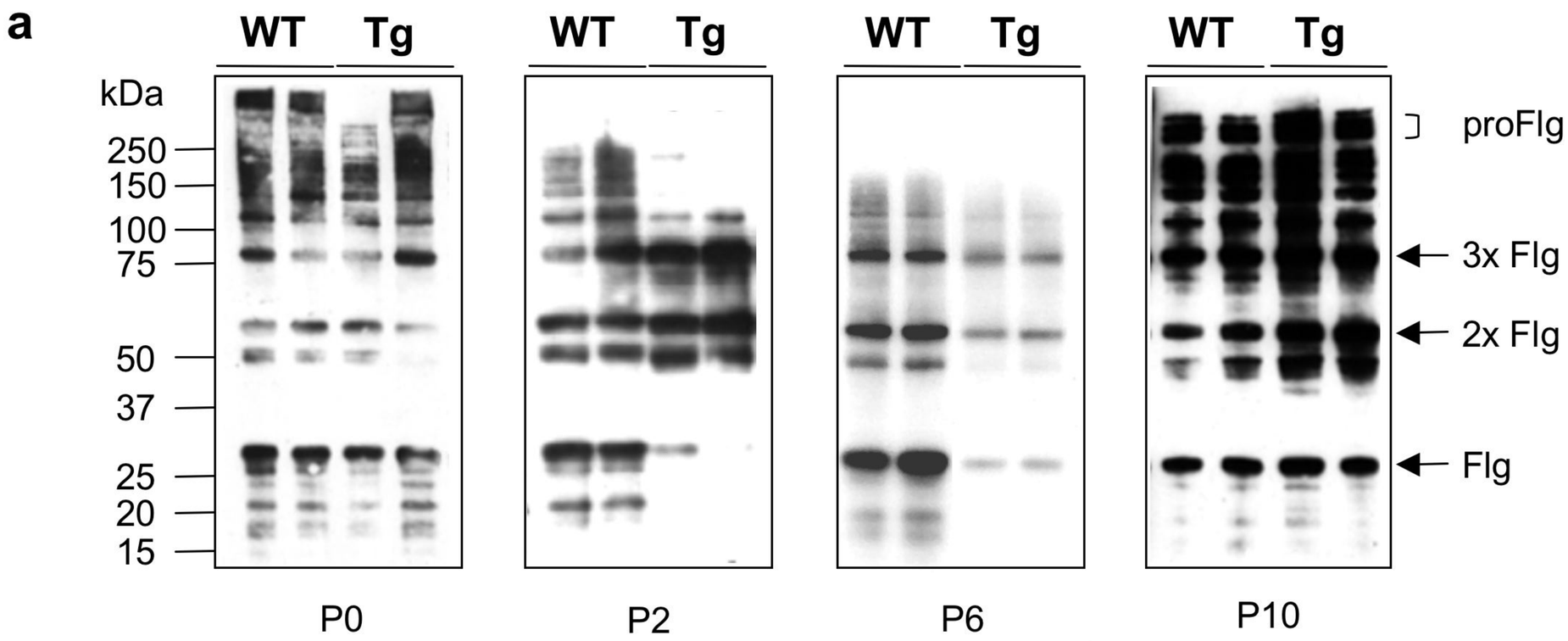

Supplementary Figure 4 – (Pro-)filaggrin expression in Tg-ELA2 epidermis and in cultured keratinocytes from Tg-ELA2

(a) Immunodetection of profilaggrin, (pro-)filaggrin processing intermediate dimers (2xFlg) and trimers (3xFlg) and filaggrin monomers (Flg) in epidermal extracts from 0-, 2-, 6- and 10-day old litters composed of 2 wild-type (WT) and 2 Tg-ELA2 animals (Tg). Tg-ELA2 epidermal extracts at days 0 and 10 showed a normal (pro-)filaggrin processing pattern. At day 2, the quantity of filaggrin monomers is dramatically decreased in Tg-ELA2 while dimers and trimers are increased. At day 6, all forms of (pro-)filaggrin are decreased in Tg-ELA2 compared to WT samples. **(b)** Relative *Flg* transcript levels in 4-day old WT and Tg-ELA2 mouse skin using quantitative RT-PCR. Transcript levels were normalized to *Hprt* abundance. Charts represent each individual value (dots) and average (histograms). n.s., not significant. **(c)** Western blot analysis showing $ELA2_{flag}$ detection produced by cultured keratinocytes from Tg-ELA2 mice. $ELA2_{flag}$ is detected in the conditioned medium and in the insoluble material of intracellular cell fraction.

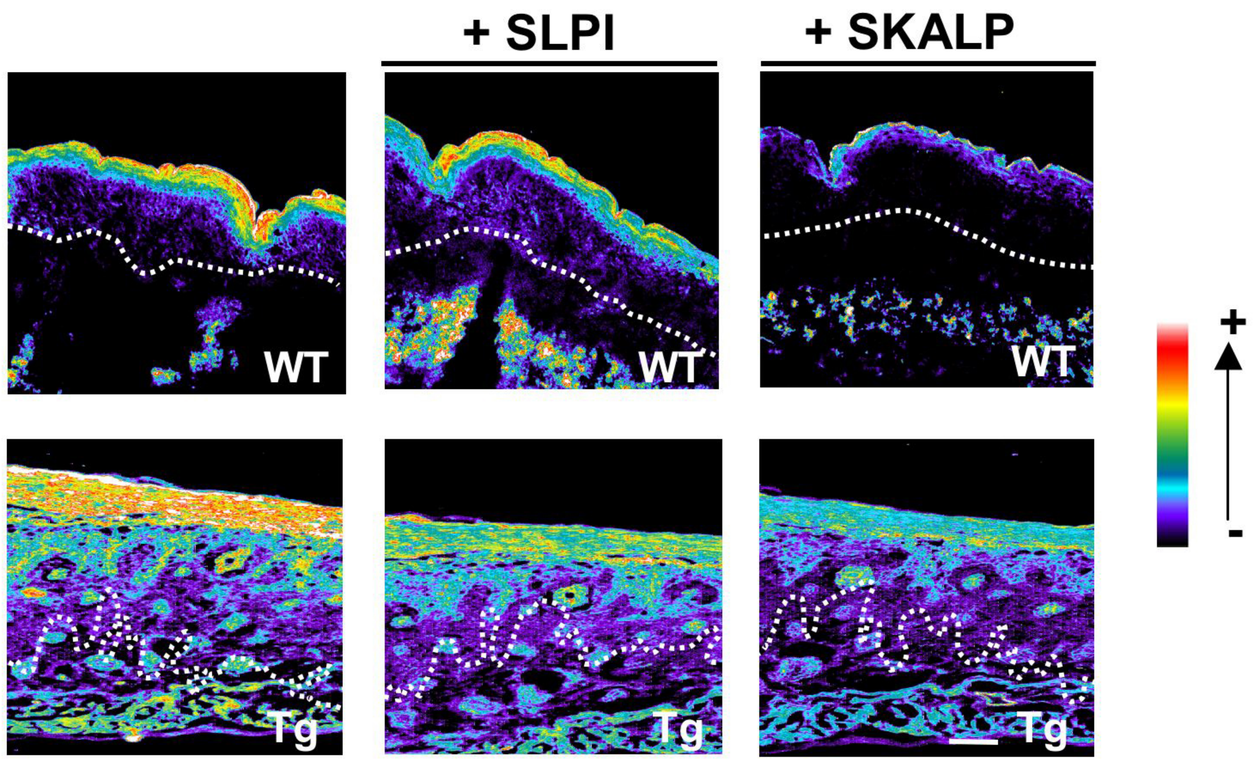

Supplementary Figure 5 - SLPI and SKALP are potent inhibitor of ELA2 activity

In situ zymography analysis showing SLPI and SKALP inhibitory capacity toward native and exogenous ELA2. Elastolytic activity of WT epidermis is mainly detected in the granular layer and stratum corneum, and is strongly enhanced in these layers of Tg-ELA2 skin. The signal intensity is slightly decreased in the presence of SLPI and markedly decreased with SKALP. The color gradient represents the intensity values of the fluorescence signals ranging from 0 (dark) to 255 (white). The dotted line represents the basal membrane of the epidermis. Scale bar: 20 μm.

Supplementary Table 1

Primers name	Forward primer (5' to 3')	Reverse primer (5' to 3')	Amplification fragment (pb)
human *ELA2* (UTR)	TTACAGAACTCCCACGGACA	CCCAGGGACTTCTTTTGGT	913
murine *Ela2*	CGTGACCTCCAGCTGCAATG	TCCTTGCCATCACCGAGTTG	194
murine *Ela2* (UTR)	ACAGACGTCCAGGGACACAC	GGGGACAGTGGCAGTAATGT	863
transgene	CAAATCAAAGAACTGCTCCTC	GTCATCGTCATCCTTGTAATC	942
Spink5 exon1	GTTCTCAAGGAGTCTAACAT	CTTGTGTGAGATAAAATGCC	400
Flg	CAATGAAGACTGGGAGGCAAGC	TGACTGGAGATGGTTTGGAGTGG	180
Hprt	CTGGTTAAGCAGTACAGCCCCAA	CGAGAGGTCCTTTTCACCAGC	65

SUPPLEMENTARY Material and Methods

Casein zymography

Skin was removed from euthanized animal and the epidermis was separated from the dermis as described22. The epidermis was crushed in 1M acetic acid solution with Ultra-turrax. After overnight extraction at 4°C, soluble proteins were lyophilized and resuspended in PBS. After acetone precipitation, proteins were assayed (Bradford, Bio-Rad) and 5 μg of soluble fractions were loaded onto casein co-polymerized with acrylamide gels (15% acrylamide, 0.05% α-casein, Sigma) for electrophoresis. Gels were washed with 2.5% Triton X-100 for 1 hour and incubated 24 hours at 37°C in a reaction buffer containing 50 mM Tris pH 8. Gels were stained with 1% Coomassie Brillant blue for 30 minutes.

Each protease inhibitor AEBSF (1 mM), pepstatin (100 μM), EDTA (15 mM), E64 (1 mM) was added to the sample before electrophoresis (15 min on ice), and in the reaction buffer.

Affinity chromatography

After overnight extraction at 4°C, soluble proteins were lyophilized and resuspended in sterile water. After acetone precipitation, proteins were resuspended in a binding buffer composed of 50 mM Tris-Cl pH7.2, 0.1M NaCl and 10 mM CaCl2. Six mg proteins were applied on 1.5 ml resin of sbTI (soybean Trypsin Inhibitor) (Pierce), a large-scale serine protease inhibitor. After overnight binding at 4°C, the resin was poured into a chromatography column, connected to a computer-monitored FPLC system (Bio-Rad Laboratories). The unfixed protein fraction (flow through) was collected for analysis. The column was washed with the binding buffer until DO_{280} was zero. The

elution buffer was obtained using a linear gradient of pH between the binding buffer and a solution composed of 0.15 M acetic acid, 10 mM CaCl2. A 30 ml gradient yielded thirty 1ml-elution fractions.

Mass spectrometry analysis

Spot excision, in-gel protein digestion, and peptide extraction

The concentrated sample was loaded onto a precast 6% acrylamide gel (Euromedex, Souffelweyershein, France). After a minimal penetration of proteins into the gel, migration was stopped and the gel was stained according to the recommendations of Silver stain kit (Amersham).

Gel slices were excised, destained with 30 mM potassium and 100 mM sodium thiosulfate (1:1, v/v) for 10 min, rinsed with deionized water for 10 min and washed twice successively with 25 mM ammonium bicarbonate for 15 min and acetonitrile.

The gel pieces were dried in a speed-vacuum centrifuge and swollen in a sufficient covering volume (25 µl) of modified trypsin (Promega) solution (20 ng/µl in 50 mM NH_4HCO_3) for 15 min at 4°C. After overnight digestion at 37 °C, three peptide extracts were performed for 15 min under shaking, once with 50 mM NH_4HCO_3 and then twice with 5% formic acid in 50% acetonitrile, respectively. The peptide mixture was concentrated to 10 µl by vacuum centrifugation.

Tandem mass spectrometry and protein identification.

The tryptic digest was analyzed by on-line capillary HPLC (Dionex/LC Peckings, USA) coupled to a nanospray Qq-Tof mass spectrometer (QSTAR Pulsar XL, Applied Biosystems, Foster City, USA). Peptides were separated on a 75 mm ID x 15 cm C18 PepMap™ column after loading onto a 300 µm ID x 5mm PepMap C18 precolumn (Dionex/LC Packings, USA). The flow rate was set at 200 nL/min. Peptides were eluted

using a 0 to 50% linear gradient of solvent B in 50 min at a flow rate of 200 nl/min delivered by the Ultimate pump (solvent A was 0.2% formic acid in 5% acetonitrile and solvent B was 0.2% formic acid in 90% acetonitrile). The mass spectrometer was operated in positive ion mode at a 2.1 kV needle voltage. MS and MS/MS data were continuously acquired in an information-dependent acquisition mode consisting of a 7s cycle time. Within each cycle, a MS spectrum was accumulated for 1s over the range m/z 300-2000 followed by three MS/MS acquisitions of 2s each on the three most abundant ions in the MS spectrum. A dynamic exclusion duration was employed to prevent repetitive selection of the same ions within 30s. Collision energies were automatically adjusted according to the charge state and mass value of the precursor ions. Mascot (version 2.2.1) was used to automatically extract peak lists from Analyst QS. wiff files. For creation of the peak lists, the default charge state was set to 2+, 3+, and 4+. MS and MS/MS centroid parameters were set to 50% height percentage and a merge distance of 0.1 amu. All peaks in MS/MS spectra were conserved (threshold intensity set to 0% of highest peak). For MS/MS grouping, the following averaging parameters were selected: spectra with fewer than five peaks or precursor ions with less than 5 cps or more than 10,000 cps were rejected, the precursor mass tolerance for grouping was set to 0.1 Da, the maximum number of cycles per group was set to 10, and the minimum number of cycles per group was set to 1. MS/MS data were searched against mammal sequences in the public database UniProt version 11.0, which consists of Swiss-Prot Protein Knowledgebase Release 53.0 and TrEMBL Protein Database Release 36.0 (233 563 entries), using the Mascot search engine (Mascot Daemon, version 2.2; Matrix Science, London, UK). Up to two trypsin missed cleavages were allowed and the mass tolerance for peptide and MS/MS fragment ions was 0.5 Da. Cysteine carbamidomethylation was set as fixed modification, methionine oxidation were

set as variable modification. The identification was confirmed by manual interpretation of corresponding MS/MS data